3D Scanning Method for Fast Motion using Single Grid Pattern with Coarse-to-fine Technique

Ryo Furukawa
Faculty of information sciences, Hiroshima City University, Japan
ryo-f@cs.hiroshima-cu.ac.jp

Hiroshi Kawasaki
Faculty of engineering, Saitama University, Japan
kawasaki@cgv.ics.saitama-u.ac.jp

Ryusuke Sagawa, Yasushi Yagi
Institute of Scientific and Industrial Research, Osaka Univ., Japan
{sagawa,yagi}@am.sanken.osaka-u.ac.jp

Abstract

An active 3D scanning method that can capture a fast motion is strongly required in wide areas. Since most commercial products using a laser projector basically reconstruct the shape with a point or a line for each scan, a fast motion cannot be captured in principle. In addition, an extended method using a structured light can drastically reduce the number of projecting patterns, however, they still require several patterns and a fast motion cannot be captured. One solution for the purpose is to use a single pattern (one shot scan). Although, one shot scanning methods have been intensively studied, they often have stability problems and their result tend to have low resolution. In this paper, we develop a new system which achieves dense and robust 3D measurement from a single grid pattern. A 3D reconstruction can be achieved by identifying grid patterns using coplanarity constraints. We also propose a coarse-to-fine method to increase the density of the shape with a single pattern.

1 Introduction

Currently active 3D scanners are widely used for actual 3D model acquisition process. Especially, coded structured light based systems have been intensively researched and commercialized, because systems of this type are relatively simple and realize high accuracy [1]. One of the significant drawbacks of the systems is that they require several patterns, and thus, a fast motion is difficult to be scanned in principle. To scan a 3D shape with fast motion, 3D scanning methods using a high-speed structured light system have been studied in recent years [5]. However, since the system still require a several frames for reconstruction, it cannot be applied to a fast motion in theory.

To overcome the aforementioned problems, 'one-shot' structured light systems that use only single images have been studied. Widely used methods in this category are embedding positional information of the projectors' pixels into spatial patterns of the projected images [7, 12]. Although the techniques can resolve the issues of rapid motions and synchronization; since multiple pixels are required to encode a single positional information into the patterns, resolution of the reconstructed shape is usually sparse. In addition, patterns of complex intensities and colors are usually used to encode positional information into local areas, the assumptions of smooth surface or simple texture is required; and if the assumptions do not hold, the decoding process of the patterns may be easily affected and leads to unstable reconstruction.

In this paper, a 3D scanning method which can capture a 3D shape with fast motion from a single image, even if the objects do not have either smooth surface or uniform texture, is presented. To achieve this, the system using a simple grid pattern formed by straight lines distinguishable only as vertical or horizontal lines and its solutions based on coplanarity constraints are utilized [4, 8]. Since the lines are required to be categorized into only two types, the image processing becomes simple and stable. In addition, there is no need to encode particular information for the local grid pattern itself, so the pattern can be dense as long as it is extractable. We also propose a coarse-to-fine technique to increase the density of the shape.

2 Related works

Shape reconstruction techniques with a structured light system, which encode positional information of a projector into temporal or spatial changes in a projected pattern, have been largely investigated and summarized in [1, 14]. A technique using only temporal changes is easy to implement, so it has commonly been used thus far [2, 6]. Since the technique uses multiple patterns necessary for decoding, it requires special attention to be applied to high-speed capturing.

Techniques using only spatial encoding of a pattern allow scanning with only a single-frame image [7, 11, 12]. They typically use complex patterns or colors for phase unwrapping process and require assumptions of smooth or continuous surface or uniform texture, either locally or globally. If the assumptions do not hold, the decoding process of the patterns may be easily affected and leads to ambiguities near depth or color discontinuities.

Several research reducing the required number of patterns using both temporal and spatial changes were presented [5, 14]. Although the technique is basically limited in that the scene must be static while multiple patterns are projected, Hall-Holt *et al.* proposed a method to alleviate the limitation by aligning the reconstructed shape with respect to a rigid body constraint [5] and Davis *et al.* proposed a method to reduce patterns by using multiple cameras [14].

Although it does not strictly involve a structured light system, methods of shape reconstruction to include movement by spatio-temporal stereo matching are proposed [3, 15, 16]. With these techniques, a projector is only used to provide a texture that changes over time for a pair of stereo cameras.

Koninckx *et al.* proposed a technique allowing dense shape reconstruction based on a single image using a simple pattern, *i.e.* a set of stripes [9, 10]. The shape reconstruction was achieved by combining dense unidentified stripes and a small number of identified

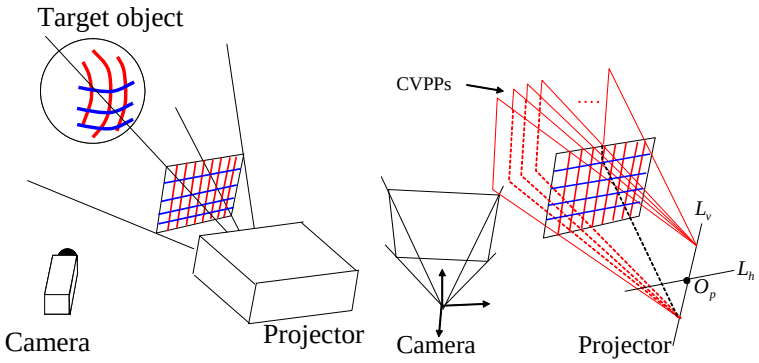

Figure 1: Scanning system:(left) the system configuration, and (right) definition of the coordinates.

stripes. Their method depends on relative numbering of the dense patterns, which assumes local smoothness of the surface and may be disturbed by shape discontinuities and line detection failures. To cope with these problems, highly sophisticated line detection and correction algorithms are presented.

Furukawa *et al.* used multiple coplanar lines projected by an uncalibrated line laser and their intersections to construct simultaneous linear equations and reconstructed a scene or shape by solving them [4]. Although, such intersections were acquired by temporally accumulated projected line-lasers on the same image plane in the method, they proposed a method which projects a grid pattern onto the target scene just one-time to retrieve all the intersections with a single frame [8]. Then, the shape reconstruction is achieved by solving the same simultaneous equations derived from the intersections. Our method is a simple extension of the method using coarse-to-fine technique. We also build an actual system to capture an extremely fast motion.

3 Shape reconstruction from grid pattern

3.1 Outline

The 3D measurement system proposed consists of a camera and a projector as shown in Fig. 1(left). Two types of straight line patterns, which are vertical and horizontal stripes, are projected from the projector and captured by the camera. The vertical and horizontal patterns are assumed to be distinguishable by color.

The straight pattern projected by the projector defines planes in 3D space. Planes defined by a vertical pattern and a horizontal pattern are respectively referred to as a vertical pattern plane (VPP) and a horizontal pattern plane (HPP).

The projector is assumed to have been calibrated. That is, all parameters for the VPPs and HPPs in 3D space are known. A VPP and a HPP with known parameters are referred to as a calibrated VPP (CVPP) and a calibrated HPP (CHPP). All the CVPPs contain a single line, as L_v in Fig. 1 (right). The same assumption holds for all CHPPs (L_v in Fig. 1 (right)). L_v and L_h share the optical center of the projector O_p. The O_p , L_v and L_h are given by calibration.

A vertical line projected onto the scene produces observable 3D curves on the surface

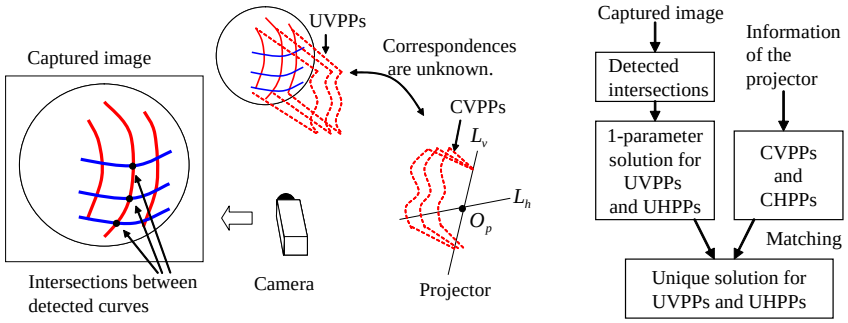

Figure 2: Planes used in the system (left) and the flow chart to estimated the planes (right).

of the scene. The 3D curves can be regarded as intersection curves between a CVPP and the scene. However, the correspondence from each of the vertical curves detected in the image to a particular CVPP that generates the curve is unknown. So, the VPP that generates a detected vertical curve is referred to as an Unknown VPP (UVPP) of the vertical curve as shown in Fig. 2 (left). An Unknown HPP (UHPP) is similarly defined.

The goal of the problem is to determine correspondences between the UVPPs (UHPPs) and CVPPs (CHPPs) (otherwise described as identifying UVPPs and UHPPs). As a result, 3D positions of all the captured intersections become known.

The outline of the proposed method is shown in Fig. 2 (right). Intersections of the vertical and horizontal curves are detected from the captured image. As described in the following section, linear equations between UVPPs and UHPPs can be obtained from the intersections of the detected curves. By solving the simultaneous linear equations obtained from the image, a one-parameter solution of the set of UVPPs and UHPPs is obtained. Using the one-parameter solution, an error function that represents the difference between the solution and the set of CVPPs and CHPPs is defined. By determining the parameter such that the error function becomes minimum, a unique solution of the UVPPs and UHPPs can be obtained.

3.2 Solving coplanarity constraints

Let the CVPPs and CHPPs be represented as $V_1, V_2, \cdots, V_M$ and $H_1, H_2, \cdots, H_N$, respectively. Also, let the UVPPs and UHPPs obtained from the captured image be represented as $v_1, v_2, \cdots, v_m$ and $h_1, h_2, \cdots, h_n$, respectively. These symbols are used to represent correspondences between UVPPs and CVPPs. In this paper, the correspondence between the k-th UVPP v_k and the i-th CVPP V_i is represented as $v_k \rightarrow V_i$, which means v_k is identified as V_i.

From the intersections of the grid pattern obtained from the captured image, linear equations can be derived. Suppose that the intersection between v_k and h_l is captured and its position on the image in the coordinates of the normalized camera is $\mathbf{u}_{k,l} = [s_{k,l}, t_{k,l}]^\top$. The planes v_k and h_l can be represented by

$$\mathbf{v}_k^\top \mathbf{x} = -1, \quad \mathbf{h}_l^\top \mathbf{x} = -1 \tag{1}$$

respectively, where 3D vectors $\mathbf{v}_k$ and $\mathbf{h}_k$ are vectors of plane parameters and $\mathbf{x}$ is a point on each plane. Note that all the intersection points detected on a single vertical curve are on a single UVPP, which is a coplanarity constraint. From the constraint, the 3D positions

of all the points on the curve fulfill equation (1). Let the 3D position of the intersection $\mathbf{u}_{k,l}$ be $\mathbf{x}_{k,l}$, then $\mathbf{x}_{k,l}$ can be represented using the coordinates of the image as

$$\mathbf{x}_{k,l} = \gamma[\mathbf{u}_{k,l}^\top \ \ 1]^\top. \tag{2}$$

By substituting $\mathbf{x} = \mathbf{x}_{k,l}$ in equation (1) and eliminating $\mathbf{x}_{k,l}$ and γ from equations (1) and (2),

$$[\mathbf{u}_{k,l}^\top \ \ 1]\,(\mathbf{v}_k - \mathbf{h}_l) = 0 \tag{3}$$

is obtained. Let the simultaneous equations of (3) for all the intersections be described as $\mathbf{Aq} = \mathbf{0}$, where $\mathbf{q} = [\mathbf{v}_1^\top, \cdots, \mathbf{v}_m^\top, \mathbf{h}_1^\top, \cdots, \mathbf{v}_n^\top]^\top$.

Let the direction vectors of the line L_v and L_h be represented as $\mathbf{l}_v$ and $\mathbf{l}_h$ respectively, and the parameters of the plane that includes both L_v and L_h be $\mathbf{p}$. Also, let the 3D coordinate vector of the optical center O_p of the projector be $\mathbf{o}_p$. UVPPs contain the line L_v, UHPPs contain the line L_h, and all the planes contain the point O_p. Thus,

$$\mathbf{l}_v^\top \mathbf{v}_k = 0, \ \ \mathbf{l}_h^\top \mathbf{h}_l = 0, \ \ \mathbf{o}_p^\top \mathbf{v}_k = -1, \ \ \mathbf{o}_p^\top \mathbf{h}_l = -1 \tag{4}$$

are obtained. Let the simultaneous equations (4) for $1 \leq k \leq m, \ 1 \leq l \leq n$ be described as $\mathbf{Bq} = \mathbf{b}$.

Since only the substitution $(\mathbf{v}_k - \mathbf{h}_l)$ appears in the equation (3), the solution of $\mathbf{Aq} = \mathbf{0}$ have freedoms of scaling and addition of a constant 3D vector. Using this fact, the general solution of $\mathbf{Aq} = \mathbf{0}$, can be written as

$$\mathbf{v}_k = s\mathbf{v}'_k + \mathbf{c}, \ \ \mathbf{h}_l = s\mathbf{h}'_l + \mathbf{c}, \tag{5}$$

where $\mathbf{q}' = [\mathbf{v}_1'^\top, \cdots, \mathbf{v}_m'^\top, \mathbf{h}_1'^\top, \cdots, \mathbf{v}_n'^\top]^\top$ is a special solution of $(\mathbf{Aq}' = \mathbf{0} \ \wedge \ \mathbf{Bq}' = \mathbf{b})$, s is an arbitrary scalar, and $\mathbf{c}$ is an arbitrary 3D vector. From $\mathbf{Aq} = \mathbf{0} \ \wedge \mathbf{Aq}' = \mathbf{0} \ \wedge \ \mathbf{Bq}' = \mathbf{b}$, $\mathbf{l}_v^\top \mathbf{c}' = 0, \ \mathbf{l}_h^\top \mathbf{c}' = 0, \ \mathbf{o}_p^\top \mathbf{c}' = -1, \ \mathbf{o}_p^\top \mathbf{c}' = -1$, where $\mathbf{c}' \equiv \{1/(1-s)\}\mathbf{c}$ is obtained. These forms indicates that the plane $\mathbf{c}'$ coincides with the plane $\mathbf{p}$. Thus, the general solution of $(\mathbf{Aq} = \mathbf{0} \ \wedge \ \mathbf{Bq} = \mathbf{b})$ can be represented as

$$\mathbf{v}_k = s(\mathbf{v}'_k - \mathbf{p}) + \mathbf{p}, \ \ \mathbf{h}_l = s(\mathbf{h}'_l - \mathbf{p}) + \mathbf{p}, \tag{6}$$

where $\mathbf{p}$ is known by calibrations and $\mathbf{v}'_k, \mathbf{h}'_l$ can be calculated from $\mathbf{A}, \mathbf{B}$ and $\mathbf{b}$. Form (6) gives the solution of the set of UVPPs and UHPPs with a free parameter s.

3.3 Determining ambiguity

The solution of the UVPPs and UHPPs of form (6) has remaining one degree of freedom. In the proposed method, the parameter s is searched to determine a unique solution such that s gives the minimum error function that estimates differences between the solution of UVPPs and UHPPs (form (6)) and the known set of CVPPs and CHPPs.

By assuming the correspondence from the k'-th UVPP to the i'-th CVPP (i.e. $v_{k'} \rightarrow V_{i'}$)

$$\mathbf{V}_{i'} = \mathbf{v}_{k'} = s(\mathbf{v}'_{k'} - \mathbf{p}) + \mathbf{p} \tag{7}$$

holds, where $\mathbf{V}_{i'}$ is the parameter vector of the CVPP $V_{i'}$. From this form, s can be calculated by

$$s = ||\mathbf{V}_{i'} - \mathbf{p}||/||\mathbf{v}'_{k'} - \mathbf{p}||, \tag{8}$$

then, all UVPPs and UHPPs are determined by using the s.

Let this s of form (8) be denoted as $s(k',i')$. Then, $\mathbf{v}_k$ and $\mathbf{h}_l$ given the correspondence $v_{k'} \rightarrow V_{i'}$, which we refer to as $\mathbf{v}_k(k',i')$ and $\mathbf{h}_l(k',i')$, respectively, can be calculated by

$$\mathbf{v}_k(k',i') = s(k',i')(\mathbf{v}_k - \mathbf{p}) + \mathbf{p}, \;\; \mathbf{h}_l(k',i') = s(k',i')(\mathbf{h}_l - \mathbf{p}) + \mathbf{p}. \tag{9}$$

The next step is comparing the calculated UVPPs (or UHPPs) with the CVPPs (or CHPPs). For each UVPP, the difference between the UVPP and the nearest CHPP is calculated as an error. Then, we can calculate the error function of the assumption $v_{k'} \rightarrow V_{i'}$ as the sum of squared errors. By searching for the minimum of the error function, we can find the optimum correspondence and solve the ambiguity.

In this paper, comparison is done based on the squared angles between the planes. For each UVPP $\mathbf{v}_k(k',i')$, an error function is defined as the angle difference between the UVPP and one of the CVPPs, where the CVPP is selected such that the angle difference becomes the minimum. Error functions of UHPPs are defined similarly. The error functions are defined as

$$\begin{aligned} e_v(\mathbf{v}_k(k',i')) &\equiv \min_{i=1,\cdots,M} \{D(\mathbf{v}_k(k',i'), \mathbf{V}_i)\}^2, \\ e_h(\mathbf{h}_l(k',i')) &\equiv \min_{j=1,\cdots,N} \{D(\mathbf{h}_l(k',i'), \mathbf{H}_j)\}^2 \end{aligned} \tag{10}$$

where D means the angle deference between two planes which can be defined as

$$D(\mathbf{v}_k, \mathbf{V}_i) \equiv \arccos((\mathbf{v}_k \cdot \mathbf{V}_i)/(||\mathbf{v}_k|| \; ||\mathbf{V}_i||)). \tag{11}$$

Thus, the error function between the set of UVPP and UHPP and the set of CVPP and CHPP is

$$E_{k'}(i') \equiv \sum_{k=1}^{m} e_v(\mathbf{v}_k(k',i')) + \sum_{l=1}^{n} e_h(\mathbf{h}_l(k',i')). \tag{12}$$

Then,

$$i'_{min} \equiv \arg\min_{i'} E_{k'}(i') \tag{13}$$

is searched, and the set of planes $\mathbf{v}_k(k',i'_{min}),\ (k = 1,2,...,m)$ and $\mathbf{h}_l(k',i'_{min}),\ (l = 1,2,...,n)$ is the unique solution.

3.4 Projection and detection of a grid pattern

The proposed method can be regarded as a "matching" between UVPPs (UHPPs) and CVPPs (CHPPs). For stable matching, adding irregularities to the arrangement of the CVPPs (CHPPs) are desirable. In this paper, combined patterns of dense vertical lines with uniform intervals and horizontal lines with random intervals as shown in Fig. 3(a) are used. Here, vertical and horizontal patterns were respectively colored red and blue so that they were distinguishable. Because of the simplicity of the projected pattern, this method is less affected by noise, surface texture, or object shape.

The detection of the curves of the grid patterns is processed as follows. First, the captured image is scanned horizontally and vertically, detecting peaks of vertical and horizontal patterns, respectively. Then, these peaks are connected using a simple labeling

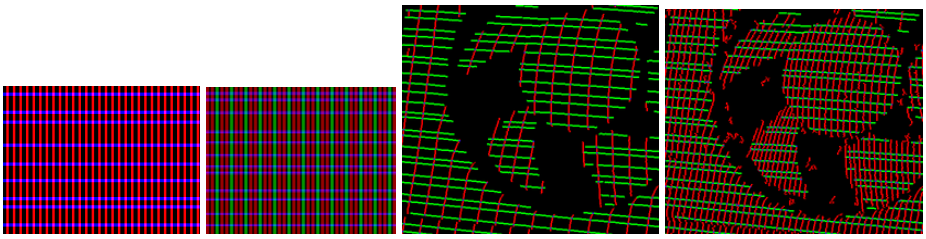

(a) (b) (c) (d)

Figure 3: projected patterns: (a) simple pattern, (b) the pattern for coarse-to-fine technique, (c) detected coarse curves and (d) detected fine curves. In (c) and (d), green curves are horizontal patterns, red curves are vertical, and intersection points are blue dots.

technique. Because of such a simple image processing, curve detection is easily affected by noise, texture color and shape of the object, however, in our experiments, above-mentioned technique sufficiently worked to retrieve satisfactory results; this is because even if the curves are disconnected by noise, if the curves are connected as network, we can still construct the same simultaneous equations.

3.5 Dense reconstruction with coarse-to-fine technique

The frequency of the projected pattern is another problem. If we need to capture the shape more densely, the higher frequency of the pattern is required. However, if we set the frequency higher than the image resolution, the correct pattern cannot be captured and the shape cannot be recovered correctly. Even if the frequency is ideal for the front face of the cylindrical shape, for example, the frequency becomes higher near the occluding boundary of the object, which resulted in the failure of the 3D reconstruction.

In this paper, we propose a simple method to solve the problem as follows. Since we use only two colors from RGB for grid patterns for identification of vertical and horizontal lines, we can use another color for another purpose. In our method, since 3D positions are reconstructed from not only the intersection points, but also all the points along detected curves, only one of the vertical or horizontal lines are required to be dense to achieve dense shape reconstruction. Therefore, we use the extra color for different frequency for vertical lines.

Figure 3 (b) shows example of the pattern and (c) and (d) show the detected lines and intersection points for sparse and dense vertical patterns respectively. In Figures, we can see that both patterns are correctly detected. To merge the reconstructed shapes from each patterns, we simply added all the recovered points.

In our implementation, we used ordinary color filter such as RGB, and thus, we can project only two different frequencies such as dense and sparse patterns. It can be easily extended to wider spectrum by using a narrow band path filter.

4 Experiments

Several experiments were conducted to demonstrate the effectiveness of the proposed method.

(a) (b) (c) (d)

Figure 4: (a) 3D scanning system, (b) the target objects and (c)(d) reconstructed shape with texture.

The first experiment was conducted to confirm the validity of the proposed method using a static object. An actual 3D scanning system was built as shown in Fig. 4 (a). Processing is performed by a PC with a Pentium Xeon 2.5Ghz CPU. The grid patterns of vertical lines with uniform intervals and horizontal lines with irregular (random) intervals were projected by a projector with a resolution of 1024×768 and scenes were captured by a CCD camera (720×480 pixels). Figures 4 (b) to (d) show the captured object and results of the Figures 4 (b)-(d) show the captured object and results of reconstruction. In the experiment, we can confirm that a ceramic bottle with texture and detailed shapes were successfully reconstructed.

Next, a scene of a box (size: 0.4 m × 0.3 m × 0.3 m) and a cylinder (height: 0.2 m, diameter: 0.2 m) was measured to test the coarse-to-fine method using the pattern proposed in section **3.5**. The scene was also measured by an active measurement method using coded structured light [13] as the ground truth. Figures 5(k) to (m) shows both the merged reconstructed shape (red and green points) and the ground truth (polygon mesh). Although there were small differences between the reconstruction and the ground truth, the correct shape was densely restored.

Finally, extremely fast motion was captured with a rotating fan as the target object. The target scene was captured with various shutter speeds as shown in Fig. 6 (b) and (c). In this case, only the fastest shutter speed 1/2550 (Figure 6 (c)) can capture the grid pattern without blur, and we can conduct the reconstruction. Figures 6 (d) to (f) show the reconstruction results. The results indicate that the proposed method successfully restored the fast motion.

5 Conclusion

This paper proposes a technique to densely measure shapes of the extremely fast motion using a single projection of a grid pattern. Since the proposed technique does not involve encoding positional information into multiple pixels or color spaces, as often used in conventional one-shot 3D measurement methods; but into a grid pattern instead, the technique is less affected by an object's texture or shape, providing robust and dense shape reconstruction. Tests were conducted to verify the method. Future work includes development of real-time capturing system and evaluation of stability and accuracy of the proposed method compared to other one-shot scanning methods.

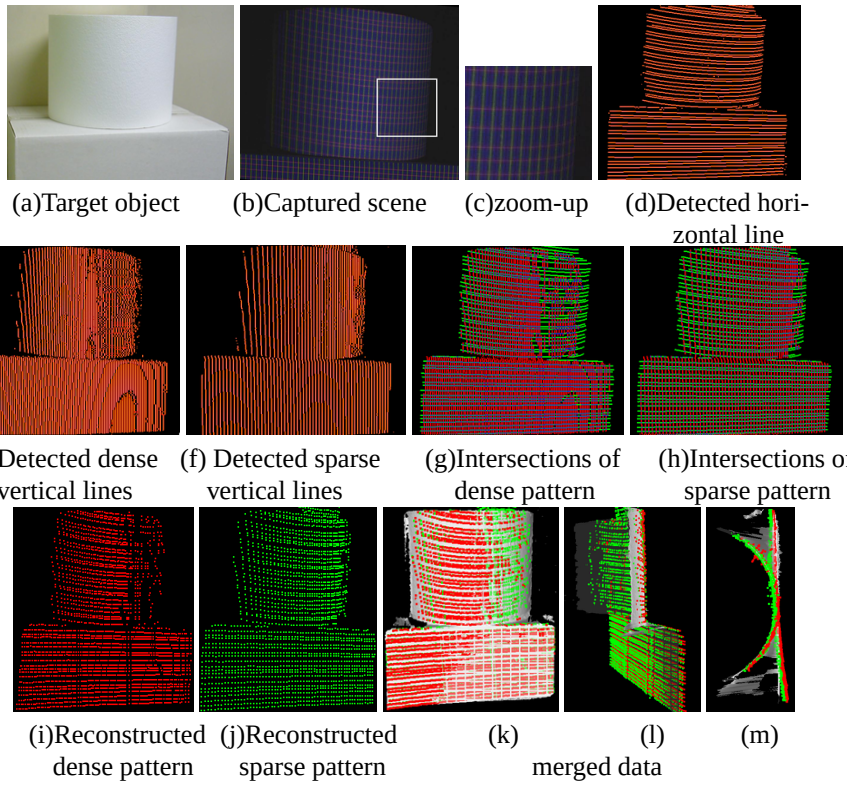

Figure 5: Detected curves and reconstruction results: in (k)(l)(m), the merged reconstructed model (red and green points) is displayed with the ground truth (shaded polygon).

Acknowledgment

This work was supported in part by SCOPE No.072103013 (Ministry of Internal Affairs and Communications, Japan) and Grant-in-Aid for Scientific Research No.19700098 and 19700157 (Ministry of Education, Science, Sports and Culture, Japan).

References

[1] J. Batlle, E. Mouaddib, and J. Salvi. Recent progress in coded structured light as a technique to solve the correspondence problem: a survey. *Pattern Recognition*, 31(7):963–982, 1998.

[2] D. Caspi, N. Kiryati, and J. Shamir. Range imaging with adaptive color structured light. *IEEE Trans. on PAMI*, 20(5):470–480, 1998.

[3] J. Davis, D. Nehab, R. Ramamoorthi, and S. Rusinkiewicz. Spacetime stereo: A unifying framework for depth from triangulation. *IEEE Transactions on Pattern Analysis and Machine Intelligence (PAMI)*, 27(2):296–302, Feb. 2005.

[4] R. Furukawa and H. Kawasaki. Self-calibration of multiple laser planes for 3D scene reconstruction. In *3DPVT*, pages 200–207, 2006.

[5] O. Hall-Holt and S. Rusinkiewicz. Stripe boundary codes for real-time structured-light range scanning of moving objects. In *ICCV*, volume 2, pages 359–366, 2001.

[6] S. Inokuchi, K. Sato, and F. Matsuda. Range imaging system for 3-D object recognition. In *ICPR*, pages 806–808, 1984.

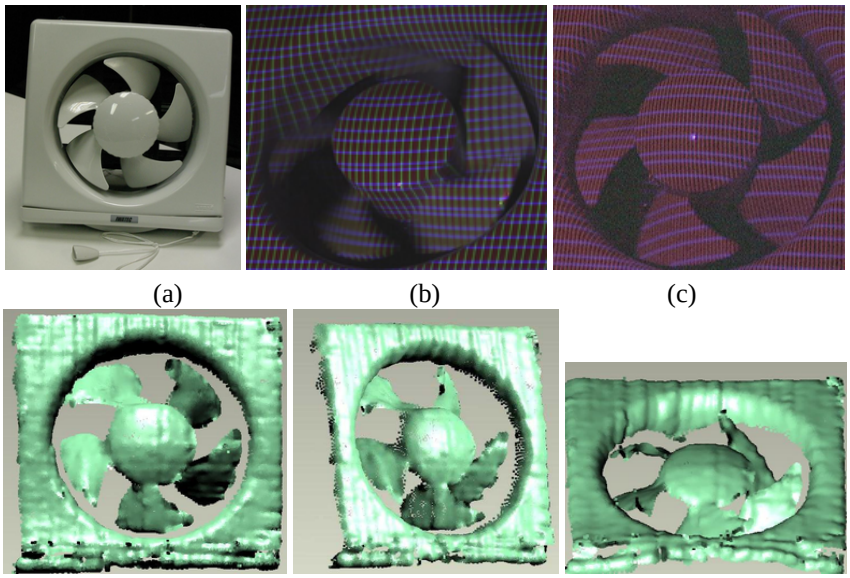

(a) (b) (c)

(d) (e) (f)

Figure 6: Reconstruction of fast rotating fan: (a) target object, (b) the captured frames with shutter speed 1/1000, (c) the captured frames with shutter speed 1/2550, and (d) to (f) reconstructed shapes.

[7] C. Je, S. W. Lee, and R.-H. Park. High-contrast color-stripe pattern for rapid structured-light range imaging. In *ECCV*, volume 1, pages 95–107, 2004.

[8] H. Kawasaki, R. Furukawa, , R. Sagawa, and Y. Yagi. Dynamic scene shape reconstruction using a single structured light pattern. In *CVPR*, pages 1–8, June 23-28 2008.

[9] T. P. Koninckx and L. V. Gool. Real-time range acquisition by adaptive structured light. *IEEE Trans. on PAMI*, 28(3):432–445, March 2006.

[10] T. P. Koninckx, T. Jaeggli, and L. V. Gool. Adaptive scanning for online 3d model acquisition. In *Sensor3D04*, pages 32–32, 2004.

[11] J. Pan, P. S. Huang, and F.-P. Chiang. Color-coded binary fringe projection technique for 3-d shape measurement. *Optical Engineering*, 44(2):23606–23615, 2005.

[12] J. Salvi, J. Batlle, and E. M. Mouaddib. A robust-coded pattern projection for dynamic 3D scene measurement. *Pattern Recognition*, 19(11):1055–1065, 1998.

[13] K. Sato and S. Inokuchi. Range-imaging system utilizing nematic liquid crystal mask. In *Proc. of FirstICCV*, pages 657–661, 1987.

[14] M. Young, E. Beeson, J. Davis, S. Rusinkiewicz, and R. Ramamoorthi. Viewpoint-coded structured light. In *IEEE Computer Society Conference on Computer Vision and Pattern Recognition (CVPR)*, June 2007.

[15] L. Zhang, B. Curless, and S. M. Seitz. Spacetime stereo: Shape recovery for dynamic scenes. In *IEEE Computer Society Conference on Computer Vision and Pattern Recognition*, pages 367–374, June 2003.

[16] L. Zhang, N. Snavely, B. Curless, and S. M. Seitz. Spacetime faces: High-resolution capture for modeling and animation. In *ACM Annual Conference on Computer Graphics*, pages 548–558, August 2004.